

# REMOTELY SENSING RUBIDIUM WITH ABSORPTION SPECTROSCOPY

Matthew Atticus Tan<sup>1</sup>, Hung Fong Bok Hillson<sup>2</sup>, Wong Wei Xiang Kendrick<sup>2</sup>  
<sup>1</sup>Anglo-Chinese School (Independent), 121 Dover Rd, Singapore 139650  
<sup>2</sup>DSO National Laboratories, 12 Science Park Drive, Singapore 118225

## Abstract

The remote sensing of rubidium is an ideal technique to determine the number density of rubidium without sample loss. Targeting the D2 transition line with a 780nm laser, absorption spectroscopy was used to determine resonant absorbance of light by rubidium vapour. The number density of rubidium was then determined using Beer-Lambert's law. To prevent saturation effects, only experimental runs with laser intensities of less than 1% of rubidium's saturation intensity was analysed. This method has proved to be viable and accurate, with the CRC empirical model relating the number density of alkali metals as functions of temperature estimating a number density within an order of magnitude. It is also able to distinguish between the isotopes of rubidium, and is likely able to work in the presence of other atoms as long as its resonant peaks (if any) does not interfere with rubidium's absorption peaks at resonance.

## 1. BACKGROUND AND PURPOSE

Accurately determining the number density of rubidium isotopes is critical, since most applications of rubidium rely on a high degree of precision. The remote sensing of rubidium prevents sample loss during measurement. Hence, this study attempts to accurately quantify the number density of rubidium remotely by the means of absorption spectroscopy targeting the D2 transition line (780nm).

## 2. THEORY

### 2.1. Energy Levels and Hyperfine Peaks

Rubidium can be excited by light, where ground state electrons ( $5s$ ) absorb a photon and promote to a higher energy level. Excitation would require an energy input (photons) corresponding to the energy difference between the ground and excited states. The energy levels of rubidium are discrete, so ground state atoms ( $5S_{1/2}$ ) can only be excited to a defined excited state ( $5P_{3/2}$ ) with a quantized amount of energy. Hyperfine splitting (Figure 1) of the D2 line ( $5S_{1/2}$  to  $5P_{3/2}$  state) results in a further splitting of the excited state. Due to the overall

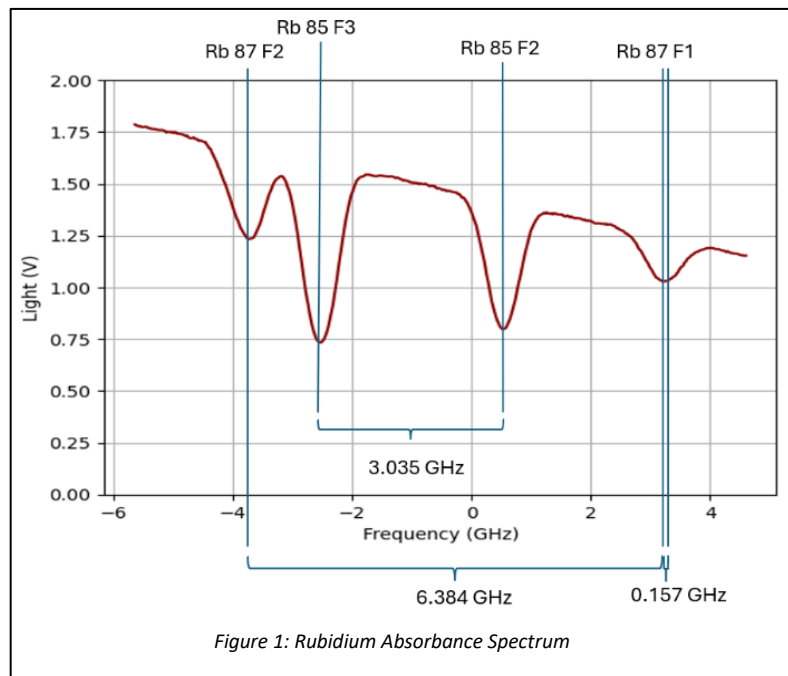


Figure 1: Rubidium Absorbance Spectrum

angular momentum of each atom ( $F$ ) being a vector sum of its nuclear spin ( $I$ ) and electron angular momentum ( $J$ ), the allowable  $F'$  states are  $F / F \pm 1$  [2]. With two initial transition states per rubidium isotope, there are 12 distinct atomic transitions.

### 2.2. Absorption Spectroscopy

Absorption spectroscopy is a technique that determines the light absorption of a medium as functions of light frequencies by measuring the intensity of light that enters and exits the medium. By probing a cell of rubidium across a range of frequencies with a 780nm laser targeting the D2 transition line, the magnitude of rubidium's absorption dips corresponding to hyperfine absorption peaks can be used to determine its number density. In contrast to the 12 distinct transitions, only four absorption dips can be resolved in the absorption spectrum (Figure 1: "Rb 87 F2", "Rb 85 F3", "Rb 85 F2", "Rb 87 F1") due to 3 transition lines being indistinguishable from each other to combine and form one absorption peak (Figure 1: An indistinguishable transition illustrated for Rb 87) [3]. The frequency spacing of these indistinguishable transition lines range from 63 – 266 MHz while the FWHM Doppler linewidth is 511 MHz. The 4 distinguishable peaks are centered around the resonant frequencies of its respective transitions and are affected by doppler and natural linewidths.

### 2.3. Doppler and Natural Linewidths

Atoms observe a frequency shift ( $\Delta f$ ) from the laser's frequency ( $f$ ) proportional to its velocity ( $v$ ) due to the doppler effect. This would result in atoms undergoing excitation and absorbing photons over a range of frequencies.

$$\frac{\Delta f}{f} = \frac{v}{c} \text{----- (Eqn. 1)}$$

Since the distribution of velocities in the line of sight of the laser is the Gaussian one-dimensional Maxwell-Boltzmann distribution, doppler broadening as a function of detuning is also Gaussian [4].  $\sigma$  which characterises the distribution was 216MHz.

$$G(f_{detuning}) = \frac{1}{\sqrt{2\pi\sigma^2}} e^{-\frac{(f_{detuning})^2}{2\sigma^2}} \text{----- (Eqn. 2)}$$

The doppler linewidth (FWHM) caused by the doppler effect is 511MHz at 295.75 Kelvin.

The natural linewidth, intrinsic to rubidium, quantifies the small range of frequencies around resonance that rubidium atoms can absorb for excitation at zero temperature.

$$L(f_{detuning}) = \frac{1}{1+4\left(\frac{f_{detuning}}{\Gamma}\right)^2} \text{----- (Eqn. 3)}$$

The distribution of atoms absorbing light at resonance as a function of detuning ( $f_{detuning}$ ) due to the natural linewidth is Lorentzian (full width half maximum ( $\Gamma$ ) = 6.0659MHz) Combining both effects, a Voigt distribution (convolution of Gaussian (Eqn. 2) and Lorentzian (Eqn. 3) profiles) as a function of detuning ( $V(f_{detuning})$ ) is obtained, accounting for doppler and natural linewidths.

### 2.4. Beer-Lambert Law

The Beer-Lambert Law describes the exponential attenuation of light, with light intensity reduction affected by the absorption cross section ( $\sigma$ ), number density ( $N$ ), and path length ( $l$ ).  $I_0$  and  $I_f$  represents the light intensity that enters and exits the rubidium cell respectively.

$$I_f = I_0 e^{-\sigma N l} \text{----- (Eqn. 4)}$$

$$\text{Rearranging equation 4, } \ln\left(\frac{I_0}{I_f}\right) = \sigma N l \text{ [5] ----- (Eqn. 5)}$$

During transitions, specific frequencies of light are absorbed by rubidium vapour to excite ground state atoms. As laser power decreases, the proportion of ground state atoms increases since less rubidium vapour is saturated. When the laser power is sufficiently low, the measured number density of ground state atoms can be approximated to be the total number density of rubidium. The absorption cross section ( $\sigma$ ) is the probability of ground state rubidium atoms absorbing photons. It is a literature value at resonance [1,7] and varies with the detuning of light. The absorption cross section as a function of detuning ( $\sigma(f_{\text{detuning}})$ ) is related to the resonant absorption cross section ( $\sigma_o$ ) by the Voigt profile ( $V(f_{\text{detuning}})$ ).

$$\sigma(f_{\text{detuning}}) = \sigma_o V(f_{\text{detuning}}) \text{ ----- (Eqn. 6)}$$

The convolution to determine the Voigt profile as a function of detuning is expressed below, with  $f'$  the variable of integration.  $g$  is defined to be central frequency of the hyperfine transition, where  $f_{\text{detuning}} = 0$ .

$$\text{Convolving equations 2 and 3, } V(g) = \int L(f') * G(g - f') df' \text{ ----- (Eqn. 7)}$$

Combining equations 5, 6, and 7, the total number density of rubidium can be given as  $N = \frac{\ln\left(\frac{I_o(g')}{I_f(g')}\right)}{\sigma_l V(g)}$ , where  $g'$  is the central frequency of the transition where detuning = 0.

## 2.5. Transmission Losses

Transmission losses could stem from reflection, absorption, and scattering by the borosilicate glass container and a layer of rubidium solid on its surface. These losses are frequency independent, causing a uniform percentage drop in light intensity across the spectrum. Hence, the light intensity exiting the rubidium cell was scaled up according to the light intensity entering the cell, resulting in absorption dips only due to rubidium vapour.

## 2.6. Number Density as determined by Temperature (1995 CRC)

In this empirical model [7], the Clausius-Clapeyron equation was used to predict the vapour pressure over the physical state of the alkali metal. Pressure is highly dependent on temperature, with vapour pressure exponentially increasing with temperature. The number density ( $[A]$ ) is then given according to the ideal gas law as a function of temperature ( $T$ ), with constants  $T_o$  (295.75 K),  $[A]_o$  ( $10^{10} \text{ cm}^{-3}$ ), and  $b$  (32.816).

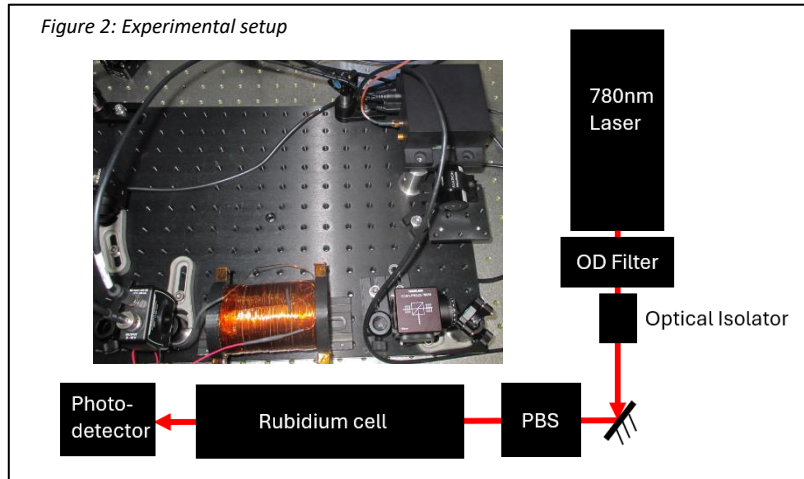
$$[A] = [A]_o \left(\frac{T_o}{T}\right) e^{(b[1-\frac{T_o}{T}])} \text{ ----- (Eqn. 8)}$$

At 297.75 Kelvin, the number density of rubidium vapour over solid was estimated as  $10^{10}$  atoms/cm<sup>3</sup>. Given so few atoms, the Van der Waals terms  $\frac{an^2}{v^2}$  and  $nb$  approach zero (Order of magnitude of  $10^{-20}$  Pa and  $10^{-17} \text{ m}^3$  respectively [8]), and ideal gas assumptions are accurate.

### 3. SETUP AND METHODS

#### 3.1. Components of the Setup

(Figure 2) A laser controlled by the CTL200 Digital butterfly laser diode controller with a 1mm radius laser beam targeting the 780nm D2 line of rubidium was used. An oscilloscope was used to modulate the frequency of the laser by varying (sweeping) the input current. A polarizing beam splitter polarized light horizontally. The rubidium cell was enclosed by a



solenoid coil, though it was not used in this study and no magnetic field was generated. A photodetector was used to measure the output light intensity.

#### 3.2. Experiments

The objective of the experiments were to determine the absorbance of rubidium over a range of laser powers.

To quantify the light intensity entering the rubidium cell given a certain laser power, the cell was removed from the setup, and optical density (OD) filters were placed between the laser and optical isolator. An amplifier was used to add gain to the weak absorption spectrums.

Next, the data from the photodetector was recorded while a light power meter was also used to measure the averaged power of the sweep.

Finally, these measurements were repeated as combinations of OD filters with increasing magnitudes were used (OD 2.0 to 5.9).

To quantify the light intensity exiting the rubidium cell, the rubidium cell was placed back between the beam splitter and photodetector. Similarly, optical density (OD) filters were placed between the laser and optical isolator. The same gain settings were applied to the amplifier according to the power of the laser.

These measurements were also repeated as combinations of OD filters with increasing magnitudes were used (OD 2.0 to 5.9).

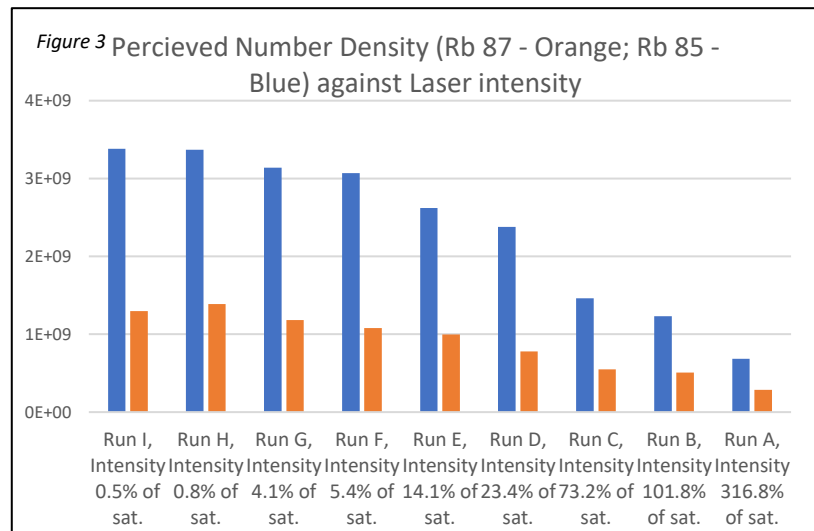
Lastly, the temperature of the rubidium cell was determined by placing a temperature probe against the rubidium cell.

## 4. RESULTS/ANALYSIS

### 4.1. Data from the Spectroscopy

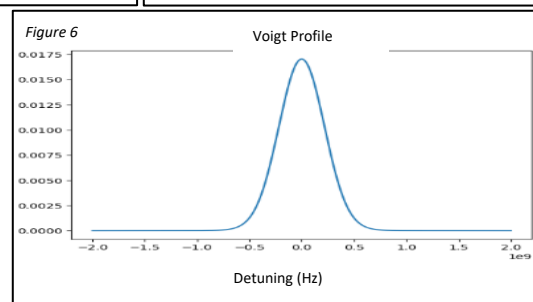
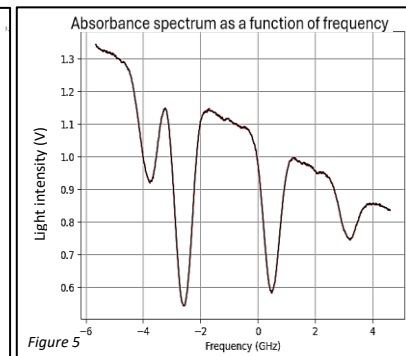
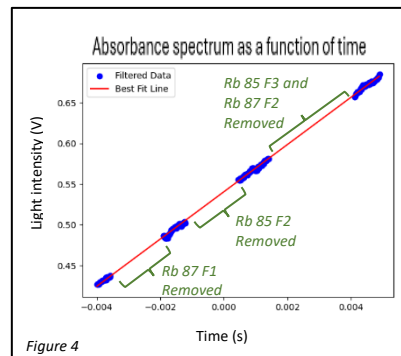
Run	OD filter	Incident light intensity (mW/cm <sup>2</sup> )
H	5.5	0.020 (0.8% of saturation intensity)
I	5.9	0.012 (0.5% of saturation intensity)

As the incident light intensity increased, the number density of rubidium was perceived to decrease due to the proportion of ground state rubidium atoms decreasing due to saturation effects (Figure 3). To avoid saturation effects, only runs H and I, with laser intensities attenuated by OD filters to be under 1% of the saturation threshold (2.5033mW/cm<sup>2</sup>) were analysed.



### 4.2. Data Processing Methods

For a given run, raw data of  $I_f$  and  $I_0$  as a function of time was cropped to focus on one frequency sweep. Data points of  $I_f(t)$  less than four standard deviations away from the center of the peak were removed (Figure 4) for  $I_f(t)$  to be assigned a uniform scaling factor to match  $I_0(t)$ .  $I_f$  and  $I_0$  was expressed as a function of frequency (Figure 5).  $V(f_{\text{detuning}})$  was obtained theoretically (Figure 6) and the maximum value (detuning = 0) was 0.0170. The total number density was then calculated with  $N = \frac{\ln\left(\frac{I_0(g')}{I_f(g')}\right)}{\sigma I 0.0170}$  where  $g'$  is the central frequency of a peak at detuning = 0.



Run	Laser Intensity (% of saturation)	Number Density of Rb 85 (cm <sup>-3</sup> )	Number Density of Rb 87 (cm <sup>-3</sup> )	Overall Number Density (cm <sup>-3</sup> )
H	0.8	$3.37 \times 10^9 \pm 2.7 \times 10^7$	$1.39 \times 10^9 \pm 2.7 \times 10^7$	$4.76 \times 10^9 \pm 3.8 \times 10^7$
I	0.5	$3.38 \times 10^9 \pm 2.7 \times 10^7$	$1.30 \times 10^9 \pm 2.7 \times 10^7$	$4.68 \times 10^9 \pm 3.8 \times 10^7$

Averaging these results, the overall number density is  $4.72 \times 10^9 \pm 1.9 \times 10^7$  atoms/cm<sup>3</sup>

## 5. DISCUSSION

### 5.1. Comparing Absorption Spectroscopy with the Ideal Gas Empirical Model

Despite the number density obtained from absorption spectroscopy and the ideal gas law being within an order of magnitude, the ideal gas law's estimate was significantly more than what was determined using absorption spectroscopy.

5.1.1. The  $e^{(b[1-\frac{T_0}{T}])}$  component of the empirical model used implied an exponential relationship between temperature and the predicted number density. This means that a relatively small variance in temperature would result in large change in number density. The fact that temperature readings were not measured during the spectroscopy, but after the experiments were over gives rise to large margin of error. For example, a  $\pm 2$  Kelvin fluctuation in temperature would result in a  $2.38 \times 10^9$  atoms/cm<sup>3</sup> change in number density.

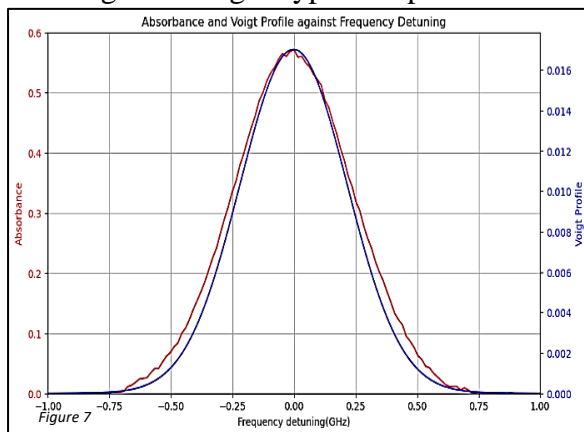
5.1.2. The empirical model (1995 CRC) used, just like other models, have a large degree of error relative to each other. For example, the Killian and Nesmeyanov models significantly deviate from not only the CRC model but also themselves [7]. For example, at 20 degrees Celsius, the Killian and Nesmeyanov models deviate by 7% and 25% from the CRC model. This suggests a considerable margin of error across the empirical model, which may contribute toward the discrepancy between the two methods of measurement.

### 5.2. Modelling the Absorption Cross Section with the Voigt Profile

The Voigt profile, determined by temperature and natural linewidth (literature), was used to model the absorbance cross section as a function of detuning in the analysis.

$$\sigma(f_{detuning}) \propto \ln\left(\frac{I_0(f)}{I_f(f)}\right)$$

Since absorbance is directly proportional to the absorption cross section, the profile also describes the distribution of absorbance as a function of detuning. Figure 7 shows the experimentally obtained absorbance ( $\ln\left(\frac{I_0}{I_f}\right)$ ) and theoretical Voigt profile as a function of detuning for a single hyperfine peak.



The experimental data (Absorbance) is seen to follow a similar general trend compared to the theoretical model (Voigt Profile) predictions. Since a 1 Kelvin increase in temperature would only increase the doppler linewidth by 0.2% and decrease the height of the peak by 0.19%, the magnitude of discrepancies regarding the linewidth of the experimental data and Voigt profile are unlikely all due to potentially inaccurate temperature measurements affecting the doppler linewidth, but attributed to inherent unknown experimental errors.

### 5.3. Potentials and Limitations of Absorption Spectroscopy

This technique can accurately differentiate the number density of different isotopes of rubidium by independently measuring the absorbance of each hyperfine peak corresponding to one isotope. It is also likely able to work in the presence of other atoms or compounds as long as its resonant peaks (if any) does not interfere with rubidium's absorption peaks at resonance.

However, this technique should only be used to quantify low concentrations of rubidium, as Beer-Lambert's law is a limiting law, with the relationship between absorbance and number density only linear at low concentrations. Additionally, the rubidium cell must have minimal and uniform reflective and absorption properties across the frequencies probed. For example, borosilicate glass has a uniform transmission rate of  $\sim 90\%$  for the range of laser detuning [9].

#### 5.4. Potential Sources of Error

Background noise (Figure 8: Prominent regions circled in red) due to light interference and imperfections with the laser is a potential source of error, resulting in irregular tiny peaks and troughs throughout the absorption spectrum. However, the effect of this error on the results is minimal, with this error affecting the averaged total number density by a mere  $\pm 1.9 \times 10^7$  atoms/cm<sup>3</sup>.



#### 6. CONCLUSION

In conclusion, absorption spectroscopy as outlined in this study is a viable and accurate technique to remotely sense the number density of rubidium at low concentrations. It is able to distinguish between the isotopes of rubidium. This technique will also likely work in the presence of other substances that do not have similar resonant frequencies as rubidium.

#### 7. ACKNOWLEDGEMENTS

The use of ChatGPT for coding debugging and development

#### 8. REFERENCES

- [1] Steck, D. A. (2001, September 25). Rubidium 87 D line data. Rubidium 87 D Line Data. <https://steck.us/alkalidata/rubidium87numbers.1.6.pdf>
- [2] V hyperfine structure of rubidium. The Charge to Mass (e/m) Ratio of Electrons. (n.d.). <https://physics.umd.edu/~beise/public/classes/p405/manual/Spring2009/Phys405-Chapter5.pdf>
- [3] Recht, J., & Kiein, W. (2010, July 3). WISC. Optical pumping of Rubidium. [https://www.physics.wisc.edu/courses/home/spring2018/407/experiments/opticalpumping/Be numof\\_AJP65.pdf](https://www.physics.wisc.edu/courses/home/spring2018/407/experiments/opticalpumping/Be numof_AJP65.pdf)
- [4] Atomic spectroscopy - spectral line shapes, etc.. NIST. (2023, March 1). <https://www.nist.gov/pml/atomic-spectroscopy-compendium-basic-ideas-notation-data-and-formulas/atomic-spectroscopy-6#:~:text=Doppler%20broadening%20is%20due%20to%20the%20thermal%20motion,7%29%20%CE%BB%20%28T%20%2F%20M%29%201%20%2F%202.>
- [5] Beer–Lambert law with Napierian Absorbance: Wolfram Formula Repository. Beer–Lambert Law with Napierian Absorbance | Wolfram Formula Repository. (n.d.-b). <https://resources.wolframcloud.com/FormulaRepository/resources/BeerLambert-Law-with-Napierian-Absorbance>
- [6] Steck, Daniel Adam. (n.d.). Rubidium 85 D line data. Rubidium 85 D Line Data. <https://steck.us/alkalidata/rubidium85numbers.pdf>
- [7] Singh, J., Dolph, P. A. M., & Tobias, W. A. (2008, April 23). Alkali Metal Vapor Pressures & Number Densities for Hybrid Spin Exchange Optical Pumping. <https://people.frib.msu.edu/~singhj/docs/vp195.pdf>
- [8] Technical data for Rubidium. Technical data for the element Rubidium in the Periodic Table. (n.d.). <https://periodictable.com/Elements/037/data.html>
- [9] Hoon, S. R. (n.d.). Optical transmission of the borofloat™ borosilicate glass window in the... | download scientific diagram. [https://www.researchgate.net/figure/Optical-transmission-of-the-Borofloat-borosilicate-glass-window-in-the-visible-and-PAR\\_fig3\\_235353465](https://www.researchgate.net/figure/Optical-transmission-of-the-Borofloat-borosilicate-glass-window-in-the-visible-and-PAR_fig3_235353465)